Journal of New Materials for Electrochemical Systems 14, 099-105 (2011)

Internal Resistance and performance of Microbial Fuel Cells: Influence of Cell Configuration and Temperature

A.L. Vazquez-Larios[1], O. Solorza-Feria[2], G. Vazquez-Huerta[2], E. Rios-Leal[1], N. Rinderknecht-Seijas[3] and H.M. Poggi-Varaldo[*,1]

[1] Environmental Biotechnology and Renewable Energies R&D Group, Dept. Biotechnology & Bioengineering, Centro de Investigación y de Estudios Avanzados del I.P.N., P.O. Box 14-740, México D.F. 07000, México
[2]Dept. of Chemistry, Centro de Investigación y de Estudios Avanzados del I.P.N. Mexico D.F., México
[3]ESIQIE del IPN, División de Ciencias Básicas, México D.F., México

Received: November 30, 2010, Accepted: February 15, 2011, Available online: April 04, 2011

Abstract: *The objectives of this work were (i) to determine the effect of electrode spacing and architecture of microbial fuel cells (MFCs) on their internal resistance (R_{int}) using two methods (polarization curve, PolC, and impedance spectroscopy, IS); and (ii) to evaluate the effect of operation temperature (35 and 23°C) of MFCs on their internal resistance and performance during batch operation. Two types of MFCs were built: MFC-A was a new design with extended electrode surface (larger ξ, specific surface or surface area of electrode to cell volume) and the assemblage or "sandwich" arrangement of the anode-PEM-cathode (AMC arrangement), and a standard single chamber MFC-B with separated electrodes. In a first experiment R_{int} of MFC-A was consistently lower than that of MFC-B at 23°C, irrespective of the method, indicating the advantage of the design A. R_{int} determined by the two methods agreed very well. The method based on IS provided more detailed data regarding resistance structure of the cells in only 10% of the time used by the PolC. R_{int} of MFC-A determined by PolC at 35°C resulted 65% lower than that of MFC-A. The effect of temperature on R_{int} was distinct, depending upon the type of cell; decrease of temperature was associated to an increase of R_{int} in cell A and an unexpected decrease in cell B. In a second experiment, the effect of temperature and cell configuration on cell batch performance was examined. Results showed that performance of MFC-A was significantly superior to that of MFC-B. Maximum volumetric power P_V and anode density power P_{An} of the MFC-A were higher than those of the MFC-B (4.5 and 2.2 fold, respectively). The improvement in P_V was ascribed to the combined effects of increased ξ and decrease of R_{int}. In spite of opposing trends in cells' R_{int}, performance of both cells in terms of $P_{V\,ave}$ improved at ambient temperature; furthermore, MFC-A outcompeted the standard cell B at both temperatures tested. The use of the new cell A would translate into a significant advantage since the power associated to heating the cells at 35°C could be saved by operation at ambient temperature.*

Keywords: internal resistance; impedance spectroscopy; microbial fuel cell; polarization curve; temperature

1. INTRODUCTION

A microbial fuel cell (*MFC*) is an electro-biochemical reactor capable of directly converting organic matter into electricity. In the anodic chamber, the microorganisms anoxically oxidize the organic matter and release electrons and protons [1,2]. Electrons are transferred to the anode that acts as an intermediate electron acceptor. The electrons flow through an external circuit where there is a resistor or a device to be powered, producing electricity and finally react at the cathode with the protons and oxygen producing water. The corresponding protons released during the oxidation of organic compounds migrate to the cathode through the electrolyte (liquor) contained in the cell and a proton exchange membrane; in this way charge neutrality is kept [3]. Electrochemical limitations on the performance of microbial fuel cells (*MFC*s) are due, *inter alia*, to the cell internal resistance (R_{int}), which results from ohmic losses caused by resistance of electrolytes (anolyte, catholyte, and proton exchange membrane (PEM)), and resistance of electrodes and connections [1,3]. Other factors such as kinetic limitation (charge-transfer resistance due to slow activation reaction rates on anode and cathode electrodes), and transport limitation (resistance

*To whom correspondence should be addressed:
Email: hectorpoggi2001@gmail.com
Phone: (5255) 5747 4324; Fax:. (5255) 5747 3313

ABBREVIATIONS

AMC	"sandwich arrangement anode-PEM-cathode
CPE_j	constant phase elements
E_{MFC}	*MFC* voltage
E_{OCP}	Open circuit potential
I_{MFC}	current intensity
IS	impedance spectroscopy
MFC	microbial fuel cell
PEM	proton exchange membrane
PolC	polarization curve
P_{An}	power density
P_{MFC}	power
P_V	maximum volumetric power
R_{ext}	internal resistance
R_{int}	internal resistance
R_j	resistance in equivalent circuits, j = 1, 2
Z_{im}	imaginary component of the impedance
Z_{re}	real component of the impedance
Greek characters	
ξ	ratio surface-of-electrode to cell volume
η_{COD}	chemical oxygen demand removal efficiency
η_{Coul}	coulumbic efficiency
ω	angular velocity

caused by retarded diffusion) [4,5] may also contribute to limited performance of *MFC*. It is of outmost importance to determine the internal resistance (R_{int}) in characterization tests of *MFC* [2]. One of the most commonly used methods is the polarization curve *(PolC)*. Yet, the impedance spectroscopy (*IS*) method is emerging as a serious candidate for the same purpose [6]. Significant improvement of *MFC* performance has come from decreasing the system's resistance through reactor architecture modifications [3,7 - 9].

Another variable that may lead to lower R_{ohmic} and thus to lower R_{int}, is a limitation of electrode area. The latter can be taken into account in the variable ξ, the ratio of surface area of electrode to the cell volume, as follows [9]:

$$\xi = A/V_{MFC} \quad (1)$$

where V_{MFC}: volume of the *MFC*, and A is the area of the electrode (usually the anode).

Since ξ is proportional to A and the R_{ohmic} is inversely proportional to A, it follows that R_{ohmic} would be inversely proportional to ξ. Beyond the math, intuitively, it is plausible that a high ξ would be desirable, since more active electrode area is available for bioelectricity generation in a given volume of the cell, that is, the exploitation of cell volume is maximized. In this regard, flat electrodes had an inherent relatively low ξ. Thus, several works have investigated the use of electrode materials with high ξ, such as granular and reticulated graphite and granular activated carbon [7, 10]. Regarding the use of flat electrodes, the ξ of the cell can still be increased if more walls of the cell are fitted with electrodes. In this way, the *MFC* fitted with a 'sandwich' ACM as reported by Liang et al. [5] might have an increased performance if the ***two*** circular surfaces of the cylindrical shell of their *MFC* were fitted with AMC arrangements.

Regarding operating temperature, most studies of *MFC* have been carried out in the mesophilic range; information related to cell operation in thermophilic or psychrophilic ranges (including ambient temperature that is usually referred as the high side of the psychrophilic range) is still relatively scarce [12,3]. Since heating the cell for operation at 35 or 55°C means an energy expenditure that could easily offset the gain due to power delivered by the cell, there is a need to gain more insight on *MFC* performance at ambient temperature. The effect of temperature on cell performance is worth investigating, since it is known that a temperature decrease might decrease the conductivity of electrolytes [12,13], increase the conductivity of metallic connections [13], decrease diffusion coefficients of chemical species in aqueous phase [14], and decrease the biochemical/biological rates [15]. Recently, the performance of a *MFC* was evaluated at different temperatures and anodic media [16]. A lag phase of 30 h occurred at 30°C which was half that at room temperature (22°C). The maximum power density at 30°C was 70 mW m^{-2} and at 22°C was 43 mW m^{-2}. At 15°C, no successful operation was observed even after several loadings for a long period of operation, The performance of electricity production from beer brewery wastewater in a single chamber membrane-free *MFC* was investigated as a function of temperature [17]. The *MFC*s could generate electricity from full-strength wastewater (2 239 mg COD L^{-1}, 50 mM phosphate buffer added) with the maximum power density of 483 mW m^{-2} (P_V = 12 mW m^{-3}) at 30°C and 435 mW m^{-2} (P_V = 12 mW m^{-3}) at 20°C, respectively. Temperature was found to have bigger impact on cathode potential than anode potential.

Thus, the objectives of this work were *(i)* to determine the effect of electrode spacing and architecture of *MFC*s on their internal resistance (R_{int}) using two methods (polarization curve, *PolC*, and impedance spectroscopy, *IS*); and *(ii)* to evaluate the effect of operation temperature (23 and 35°C) of *MFC*s on their internal resistance and performance during batch operation.

2. MATERIALS AND METHODS

2.1. Microbial fuel cell architecture

Both *MFC* consisted of a horizontal cylinder built in Plexiglass 78 mm long and 48 mm internal diameter, according to what was reported elsewhere [9]. In summary, in the *MFC*-A (new design), the two circular, opposing faces of the cylindrical shell were fitted with corresponding sets of an assemblage or circular "sandwich" arrangement that consisted (from inside to outside) of an anode made of Toray carbon cloth, the proton exchange membrane (Nafion 117), the cathode made of flexible carbon-cloth containing 0.5 mg/cm^{-2} platinum catalyst (Pt 10 wt%/C-ETEK), and a perforated plate of stainless steel 1 mm thickness. This "sandwich" arrangement is referred to as *AMC* for the anode-membrane (PEM)-

cathode.

On the other hand, the standard cell *MFC-B* was fitted with a circular anode made of stainless steel plate 1 mm thickness with a Toray flexible carbon-cloth sheet placed in one circular face and a cathode in the opposing face made of (from inside to outside): proton exchange membrane (Nafion 117), a Toray flexible carbon-cloth containing 0.5 mg/cm^{-2} platinum catalyst (Pt 10 wt%/C-ETEK), and a perforated plate of stainless steel 1 mm thickness. All the cathodes in both cells *MFC-A* and *MFC-B* were in direct contact with atmospheric air on the perforated metallic plate side.

2.2. Experimental design

2.2.1. First experiment: Electrochemical characterization by polarization curve and impedance spectroscopy

The electrochemical characterization of both cells was performed by *PolC* at both temperatures 23 and 35°C according to procedures described by Poggi-Varaldo et al. [2], whereas the characterization by *IS* was carried out at 23°C [6].

2.2.2. Second experiment: Effect of temperature on performance microbial fuel cells

After characterization, batch operation of microbial fuel cells was carried out as follows: the *MFC*s were loaded with substrate and inocula (see below) and batch-operated for 50 h at 23°C and 35°C, without mixing. The circuit of each *MFC* was fitted with a corresponding external resistance equal to the R_{int}, in order to be consistent with the Theorem of Jacobi [18] that states that a cell delivers maximum power when the load resistance (external) is equal to the R_{int}. The cells were loaded with 143 mL of mixed liquor from a sulphate-reducing and 7 mL of a model extract similar to that produced in the biological hydrogen production from the organic fraction of the municipal solid wastes as shown below. The initial COD and biomass concentration in the cell liquor were *ca.* 1 250 mg O_2 L^{-1} and 890 mg VSS L^{-1}, respectively.

2.3. Organic Fuel and Inocula

The organic fuel of the cells were 7 mL of a model leachate, similar to that produced in the biological hydrogen production from the organic fraction of the municipal solid wastes [19-21]. The model extract was concocted with a mixture of the following substances (in g L^{-1}): acetic, propionic and butyric acids (4 each) as well as acetone and ethanol (4 each) and mineral salts such as $NaHCO_3$ and Na_2CO_3 (3 each) and K_2HPO_4 and NH_4Cl (0.6 each). Organic matter concentration of model extract was *ca.* 25 g COD L^{-1}. The cells were loaded with 143 mL of mixed liquor from a sulphate-reducing, mesophilic, complete mixed, continuous bioreactor. The bioreactor had an operation volume of 3 L and was operated at 35°C. The bioreactor was fed at a flow rate of 120 ML d^{-1} with an influent whose composition was (in g L^{-1}): sucrose (5.0), glacial acetic acid (1.5), $NaHCO_3$ (3.0), K_2HPO_4 (0.6), Na_2CO_3 (3.0), NH_4Cl (0.6), plus sodium sulphate (7.0). The initial COD and biomass concentration in the cell liquor were *ca.* 1 250 mg O_2 L^{-1} and 890 mg VSS L^{-1}, respectively.

2.4. Polarization curves and impedance spectroscopy

The *PolC* procedures were similar to that reported elsewhere [2]. In short, the circuit of the *MFC* was fitted with an external, variable resistance device. In this regard, we carried out the polarization curve of the *MFC*, relating mathematically the cell voltage (E_{MFC}) and current intensity (I_{MFC}) against the external resistance value, forwards and backwards regarding the R_{ext} values. *Ab initio*, the *MFC* was operated at open circuit for 1 h. Afterwards, the R_{ext} was varied from 1 000 Ω to 10 kΩ and viceversa. After this, the cell was set to open circuit conditions for 1 h in order to check the adequacy of the procedure (values of initial and final open circuit voltages should be close). The voltage was measured and recorded with a Multimeter ESCORT 3146A.

The impedance measurements were performed within the frequency range from 2 MHz to 10 mHz, at the open circuit voltage (E_{OCP}) and using a two-electrode configuration. The amplitude of the superimposed signal perturbation was $\pm$10 mV. Previous to impedance measurements 30 minutes were allowed for establishing a pseudo steady-state. The impedance measurements were performed in a potentiostat/galvanostat Voltalab model PGZ402. In order to simulate the impedance response two equivalent circuits were used [6].

2.5. Analytical methods and calculations

The COD and VSS of the liquors of sulphate-reducing seed bioreactor and cells were determined according to the Standard Methods [22]. In addition, the individual concentrations of volatile organic acids and solvents in the model extract were analyzed by gas chromatography in a chromatograph Perkin Elmer Autosystem equipped with a flame ionization detector as described elsewhere [19].

For the standard cell the parameter ξ (ratio of electrode surface area to cell volume) was estimated as:

$$\xi_B = (pD_e^2/4)/(pD_e^2\, L/4) = 1/L = 13\ m^{-1} \quad (2)$$

where D_e is the diameter of the electrode (either anode or cathode); L is the geometric height of the cylindrical cell.
On the other hand, for the *MFC*-A new design cell the ratio was:

$$\xi_A = 2(pD_e^2/4)/(pD_e^2\, L/4) = 2/L = 26\ m^{-1} \quad (3)$$

That is, the relationship between ξ of both cells:

$$\xi_A/\xi_B = 2 \quad (4)$$

The current (I_{MFC}), power (P_{MFC}), power density (P_{An}) and volumetric power (P_V) were calculated as previously described [2]. The η_{Coul} is the ratio between the actual amount of produced electrons *(CRS)* to the electrons that could be produced from the substrate *(CTS)*, as it follows:

$$\eta_{Coul}(\%) = \frac{CRS}{CTS} \cdot 100 \quad (5)$$

$$CRS = \int_0^t I_{MFC}\, dt \quad (6)$$

$$CTS = \frac{F_i \cdot b_{COD} \cdot \left(COD_i - COD_f\right) \cdot V_{MFC}}{M_{COD}} \quad (7)$$

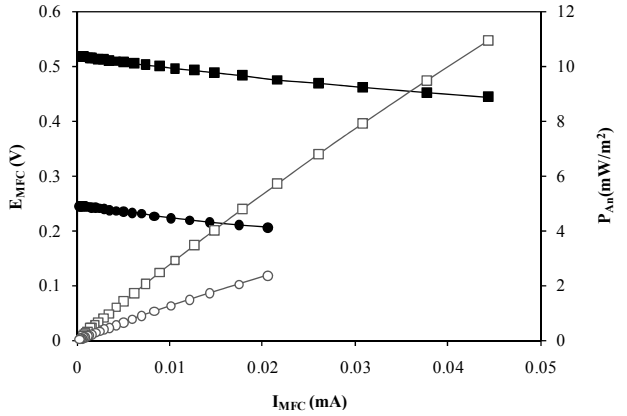

Figure 1. Curves of polarization (■, new design *MFC-A*; ●, standard *MFC-B*) and power densities (□, new design *MFC-A*; ○, standard *MFC-B*) of microbial fuel cells using a sulphate-reducing inoculums at 23°C.

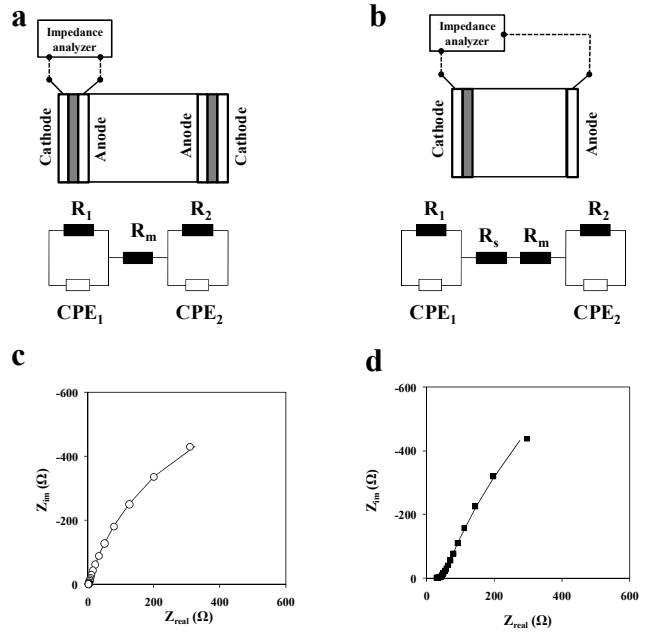

Figure 2. Equivalent circuits for (a) new type *MFC-A*, (b) standard *MFC-B*, (c) Nyquist plot of impedance spectra of *MFC-A*, (d) Nyquist plot of impedance spectra of *MFC-B*. Characterization tests run at 23°C. R_s is the solution resistance, R_m is the resistance of the membrane, R_1 is the charge transfer resistance at the anode, R_2 is the charge transfer resistance at the cathode, CPE_1 accounts for double-layer capacitance of porous electrode at the anode and, CPE_2 stands for double-layer capacitance at the cathode.

where F: Faraday's constant (96 485 Coulombs mol^{-1} e^-), b_{COD}: number of moles of electrons harvested from the *COD* (4 mol e^- per mol of *COD*), COD_i: initial *COD* (g L^{-1}), COD_f: final *COD* (g L^{-1}), V_{MFC}: *MFC* operation volume (L), M_{COD}: *COD*'s molecular weight (32 gmol^{-1}).

3. RESULTS AND DISCUSSION

3.1. First experiment

3.1.1. Electrochemical characterization by polarization curve and impedance spectroscopy at 23°C

Values of R_{int} obtained from the *PolC* method were 1 750 and 2 100 Ω for *MFC-A* and *MFC-B*, respectively (Table 1). Internal resistances determined by linear regression were associated to high values of coefficient of determination in the range 0.9548 - 0.9944, i.e., the regressions were significant. The corresponding maximum area power densities P_{An} were 10.9 and 2.4 mW m^{-2}, whereas the volumetric power values P_V corresponded to 131 and 28 mW m^{-3} for cells A and B, respectively (Fig. 1). On the other hand, Fig. 2 shows the Nyquist diagrams of *MFC-A* and *MFC-B*, in both cases the plots present one incomplete semicircle, however as it will be describe below, many electrochemical processes are involved in this single loop. In order to obtain quantitative information from the impedance spectra, two electric circuits were employed. The electric circuit in Fig. 2a was used to simulate the impedance response of new type *MFC-A*, while the electric circuit in Fig. 2b was used for standard *MFC-B*. The constant phase element in , *CPE*, improves the quality of the fit, while using a simple ideal two-plate capacitor produces poor results. The impedance of *CPE* is defined as $Z_{CPE} = 1/[(jw)^n Q]$), where j is the complex number, w the angular frequency, Q is related with the capacitance of the double layer (C_{dl}), n compensates the non-homogeneity of the system due to the roughness of the electrode, R_s is the solution resistance, R_m is the resistance of the membrane, R_1 is the charge transfer resistance at the anode, R_2 is the charge transfer resistance at the cathode, CPE_1 accounts for double-layer capacitance of porous electrode at the anode and, CPE_2 stands for double-layer capacitance at the cathode [23]. The R_{int} is defined as the sum of all resistances, i.e. $R_{int}=R_1+R_m+R_2$ in the case of *MFC-A* and $R_{int}=R_1+R_m+R_s+R_2$ in the case of *MFC-B* (see Figure 2a and 2b). The impedance spectra of new type *MFC-A* and standard *MFC-B* were fitted using ZView2™ program. By using this program, the values of all the components of electric circuits (Figure 2c and 2d) were obtained. The R_{int} values for *MFC-A* and *MFC-B* were 1 570 and 2 685 Ω, respectively. The values of R_{int} of each cell by the different methods were in reasonable agreement (Table 1); the differences in R_{int} between methods were 10% and -32% for the cells type A and type B, respectively, taking the *PolC* values as reference. On average, the R_{int} of the *MFC-A* was significantly lower (*ca.* 30%) than that of *MFC-B*. The improvement of P_{An} and P_V of cell A was ascribed to the combined effects of decreasing R_{int} due "sandwiching" of the electrodes and the increase of ξ. The *IS* provided more detailed data regarding resistance structure of the cells in only 10% of the time used by the *PolC* method.

Table 1. Internal resistance of the cells for polarization curve and impedance spectroscopy at 23°C.

Method	R_{int} (Ω)	
	MFC-A	*MFC-B*
Polarization curve	1 750 ± 41	2 040 ± 42
Impedance spectroscopy	1 570 ± 124	2 685 ± 240

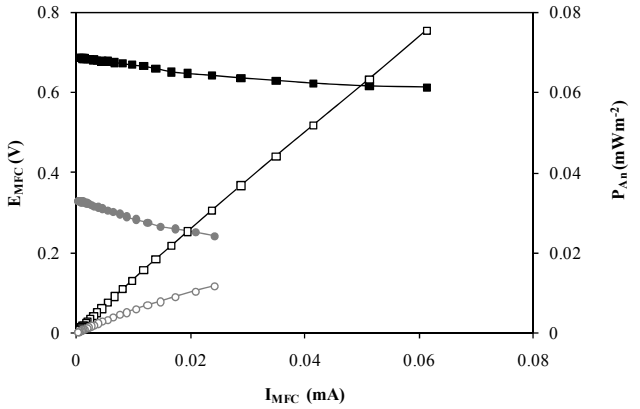

Figure 3. Curves of polarization (■, new design *MFC-A*; ●, standard *MFC-B*) and power densities (□, new design *MFC-A*; ○, standard *MFC-B*) of microbial fuel cells using a sulphate-reducing inoculums art 35°C.

3.1.2. Polarization curves of Microbial Fuel Cells at 35°C

PolC were very close to straight lines; the internal resistances were estimated from the slopes of the corresponding regression lines as 1 360 ± 86 and 3 900 ± 130 Ω for *MFC-A* and *MFC-B*, respectively (Fig. 3), i.e., a factor of 2.9 between resistances of B and A, or a 65% decrease of $R_{int,A}$ with respect to $R_{int,B}$. just due to type of cell.

In particular, the proportion of R_{int} decrease in our work was similar to the 68% reduction in R_{int} value reported by Liang et al. [5] in a comparative study of a single chamber *MFC* fitted with a "sandwich" *AMC* and a second cell where the electrodes were separated 4 cm. Maximum density powers generated by *MFC-A* and MFC-B at 35°C in our work were 20.9 y 3.3 mW m^{-2}, respectively, that is, 6.4-fold superior for MFC-A.

On the other hand, the effect of temperature decrease on R_{int} was distinct in both cells: R_{int} of *MFC-A* was higher at 23°C (increased by 29%) whereas R_{int} of *MFC-B* was significantly lower at 23°C (decrease by 48%). To some extent, R_{int} values of both cells tended to level-off at 23°C (1750 and 2040 Ω for cell A and cell B, respectively.).

The pattern of resistance variation with temperature in *MFC-A* is in agreement with several criteria based on electrochemical, transport phenomena, and biological arguments. Electrolyte conductivities tend to decrease with a decrease of temperature. For most ions in water solution, the value of the ionic equivalent conductivity increases with temperature by about 2.2-2.5 %/°C or K [12,13]. This temperature dependence seems to be the result of the decrease of water viscosity with temperature increase, which is of the same order (2%/°C or K). Temperature coefficients of H^+ and OH^- are slightly lower, 0.014 and 0.016, respectively.

For instance, maximum ion mobilities if hydronium ion, sodium ion, chloride, and acetate are 339.9, 48.0, 73.4, and 39.2 at 23°C, whereas the corresponding values at 35°C are 397, 61.5, 92.2, and 49.3 cm^2 (ohm. g-equiv)$^{-1}$, respectively [13]. On the other hand, dynamic viscosity of water is 0.937 and 0.719 cpoise at 23 and 35°C, respectively. Furthermore, the product of ionic conductivity times the dynamic viscosity is fairly constant with temperature, as predicted by the equation of Stokes [13].

In contrast, conductivity of solid conductors decreases with temperature increase; so, its contribution to ohmic resistance seems to decrease at lower temperature [13].

In liquid solution, difussivity coefficients are proportional to the absolute temperature (Wilke's correlation based on the Stokes-Einstein equation, [14]) *i.e.*, mass transfer by diffusion increases with temperature. Yet, this effect amounts to only 4% variation of the coefficient in the temperature range 23-35°C. Also, it is well

Table 2. Average performance of microbial fuel cells during batch operation in this work.

Parameter	35°C		23°C	
	MFC-A	*MFC-B*	*MFC-A*	*MFC-B*
R_{ext} (Ω)	1 300 [a]	3 900 [a]	1 700[a]	2 100[a]
$P_{An\text{-}max}$ (mWm^{-2})	38.43	4.63	29.67	13.29
$P_{V\text{-}max}$ (mWm^{-3})	922.2	69.8	712.0	159.4
$E_{MFC\text{-}max}$ (V)	0.29	0.20	0.30	0.22
$I_{MFC\text{-}max}$ (mA)	0.24	0.05	0.18	0.11
$P_{MFC\text{-}max}$ (mW)	0.14	0.01	0.10	0.02
$P_{An\text{-}ave}$ (mWm^{-2})	20.0 ± 1.9	4.6 ± 0.4	25.3 ± 4.8	7.5 ± 1.4
$P_{V\text{-}ave}$ (mWm^{-3})	479.6 ± 23.1	55.6 ± 4.7	606 ± 57.5	90.5 ± 23.1
$E_{MFC\text{-}ave}$ (V)	0.21 ± 0.01	0.18 ± 0.01	0.28 ± 0.03	0.16 ± 0.02
$I_{MFC\text{-}ave}$ (mA)	0.17 ± 0.03	0.04 ± 0.002	0.16 ± 0.02	0.08 ± 0.02
$P_{MFC\text{-}ave}$ (mW)	0.072 ± 0.003	0.0083 ± 0.0007	0.091 ± 0.009	0.014 ± 0.001
η_{COD} (%)	35	38	32	37
η_{Coul}(%)	4	1	5	2

Notes: [a] the external resistances were set at these values for cell operation; R_{ext}, external resistance; P_{An}, surface area power density; P_V, volumetric power; E_{MFC}, cell voltage; I_{MFC}, cell current intensity; P_{MFC}, power delivered by the cell; η_{COD}, organic matter removal efficiency as *COD*; η_{Coul}, coulombic efficiency. Subindices: max, maximum; ave, average.

known that biochemical reaction rates of the most commonly found microorganisms increase with temperature in the ambient-mesophilic range [15]. That is, the increase of R_{int} at 23°C of cell A is consistent with three out of four arguments (electrolyte resistance increase, lower diffusion, low biochemical rates).

In contrast, the decrease of R_{int} and improvement of power with temperature decrease in cell B is in contradiction with those lines of arguments. To the best of our knowledge, we could not find a plausible explanation for this unexpected result.

3.2. Second experiment

3.2.1. Effect of temperature on performance microbial fuel cells at 23 and 35°C

The maximum volumetric power ($P_{V\,max}$) decreased from 922 and 712 mW m^{-3} when the *MFC-A* was operated at 35 and 23°C, respectively. On the other hand, $P_{V\,max}$ of *MFC-B* increased from 70 to 159 mW m^{-3} with temperature decrease (Table 2). These crossed variations of $P_{V\,max}$ and $P_{V,ave}$ paralleled inverse crossed variations of internal resistances with temperature (see section 3.1). Contrary to what was expected, average performance in terms of $P_{V\,ave}$ was better at 23 than at 35°C for both cells (Table 2). This could be due to a higher voltage output of the cell A at 23°C than at 35°C, that could offset the negative effect of resistance increase (Table 2). This result is very significant, since the energy expenditure to heat the cells for operation at 35°C could be saved by operating at ambient temperature.

In the batch operation, performance of the new design *MFC-A* was superior to that of *MFC-B* as revealed by higher power outputs (Table 2). Maximum volumetric power P_V and anode density power P_{An} of the *MFC-A* were superior to those of the *MFC-B* by factors of 4.5 and 2.2, respectively (Table 2). The improvement in P_V was probably due to the combined effects of increased ξ and lower R_{int} in cell A. Yet, it is interesting to note that the expected (algebraic) enhancement due these two features would be in the order of 2.4 ((2/1)*(2 040 W/1 700 W) = 2.4), that is, the experimental improvement factor was almost double of the mere algebraic one. One may speculate that there was a synergistic effect between the architecture of the cell (ξ and *AMC*) and the lower internal resistance of the 'sandwich' *AMC* arrangement on the volumetric power of the *MFC*.

A 3-fold increase in density power P_{An} of a 'sandwich'-*AMC MFC* over that of a *MFC* with separated electrodes was reported by Liang et al. [5]; the improvement factor was lower than the factor 4.5 determined in our work. Yet, their absolute values of power density [5] were much higher than those found in the present work.

The P_{An}, P_V , and η_{Coul} of *MFC-A* at 23°C in this work were superior by factors of 2 to 3 (depending on the response variable) to those reported in a previous work [2] that carried out experiments at 35°C with a single chamber *MFC* fitted with separated electrodes and loaded with sulphate-reducing inoculum and an influent similar to the used in the present research.

There was not a significant effect of temperature on the overall coulombic efficiencies, although the type of cell gave a significant difference in favor of *MFC-A* (4 to 2.5 fold), (Table 2). Variation due to temperature of $P_{V,max}$ and $P_{An,max}$ of *MFC-A* was consistent with previous research [24] that have found a decrease of power delivered with temperature decrease, probably due to combined effects of lowered biological activity and increased electrolyte resistance at lower temperatures. Yet, *MFC-B* in our work showed an unexpected response with temperature, as discussed above.

The P_V of the *MFC-A* was in the middle to high side of the range of P_V reported in the literature. Yet, the P_{An} of the *MFC-A* was in the low range of published results [1,5,25] that showed a predominance of studies using simple substrates (such as glucose, acetate), anaerobic inocula or seed from municipal wastewater, and even use of Pt in the electrodes and connections [25,26]. Low values of power densities obtained in this work could be due to the fact that our cell architecture relied on a cell design with a relative large volume compared to other designs [27-29].

Also, platinum at low concentration was used as a catalyst only at the cathode to facilitate the final reaction to produce water in our study; yet, the external circuit lacked platinum. Another possible factor could be lack of acclimation of the inoculum to the new substrate. The microbial consortium in the sulphate-reducing inoculating bioreactor was acclimated to a substrate that consisted of sucrose and acetic acid, as well as sodium sulfate as electron acceptor. After transferring to the *MFC*, the substrate fed was a model extract that neither contained sucrose nor sulphate (the substrate was a mixture of acetic, propionic and butyric acids as well as acetone and ethanol and mineral salts.) That is, the absence of acclimation to the new substrate could have played a negative effect on *MFC* performance. Furthermore, the inoculum was not previously enriched for electrochemically-active bacteria (also known as anodophilic or exoelectrogenic bacteria). As it is known, most of these microorganisms are dissimilatory metal reducing microorganisms, and their presence and predominance in the consortia anchored in *MFC*s are associated to high power outputs [30-32].

Organic matter removal was low to moderate: 35 and 32% in the *MFC-A*, 38 and 37% in the *MFC-B* at 35 and 23°C, respectively (Table 2). These results were consistent with low values of the η_{Coul}. Both parameters could be increased by increasing the time of operation (since at the end of the batch run most of the organic substrate was still available), by further lowering the internal resistance of the cell, and by using inocula previously enriched in electrochemically-active bacteria [30-33].

4. CONCLUSIONS

Values of R_{int} of each cell by the different methods of determination were in reasonable agreement; the differences in R_{int} between methods were 10% and -28% for the cells type A and type B, respectively. On average, the R_{int} of the *MFC-A* was significantly lower (*ca.* 31%) than that of *MFC-B* at 23°C. The *IS* provided more detailed data regarding resistance structure of the cells in only 10% of the time used by the *PolC* method.

A new design of *MFC* whose main features were the assemblage or "sandwich" arrangement of the anode-PEM-cathode and the extended surface area of electrodes (higher ξ) exhibited a performance significantly superior to that of a standard cell where the electrodes were separated. Several parameters indicated an unexpected positive effect of temperature decrease on *MFC-B* (decrease of R_{int}, increases of P_{An} and P_V). In contrast, temperature decrease had a negative effect on several parameters of *MFC-A* (increase of R_{int}, decreases of $P_{An\,max}$ and $P_{V\,max}$). In spite of this, performance of both cells in terms of $P_{V\,ave}$ improved at ambient temperature; furthermore, $P_{V,ave}$ of *MFC-A* was still superior to that of the standard cell B at both temperatures tested. The use of the new cell A would

translate into a significant advantage, since the power associated to heating the cells at 35°C could be saved by operation at ambient temperature.

5. ACKNOWLEDGEMENTS

ICYTDF and CINVESTAV-IPN (Mexico) partial financial support to this research is gratefully acknowledged. ALV-L received a graduate scholarship from CONACYT, Mexico. The authors wish to thank the Editor, Associate Editor, and Referees, for their proactive comments that allowed for significant improvement of the manuscript. The excellent help with chromatographic analysis of Mr. Cirino Rojas of Central Analítica, Dept. Biotechnology and Bioengineering, CINVESTAV del IPN, the technical assistance of Mr. Rafael Hernández-Vera from the Environmental Biotechnology and Renewable Energy R&D Group and personnel from the Fuel Cell and Hydrogen Group of CINVESTAV is much appreciated.

REFERENCES

[1] B.E. Logan, B. Hamelers, R. Rozendal, U. Schröder, J. Keller, S. Freguia, P. Aelterman, W. Verstraete, K. Rabaey, Environ. Sci. Technol., 40, 5181 (2006).

[2] H.M. Poggi-Varaldo, A. Carmona-Martínez, A.L. Vázquez-Larios, O. Solorza-Feria, J. New Mater. Electrochem. Syst., 12, 49 (2009).

[3] H. Rismani-Yazdi, S.M. Carver, A.D. Christy, O.H. Tuovinen, J. Power Source, 180, 683 (2008).

[4] Z. He, N. Wagner, S.D. Minteer, L.T. Angenent, Environ. Sci. Technol. 40, 5212 (2006).

[5] P. Liang, X. Huang, M-Z Fan, X-X Cao, C. Wang, Appl. Microbiol. Biotechnol., 77, 551 (2007).

[6] S. Ouitrakul, M. Sriyudthsak , S. Charojrochkul , T. Kakizono, Biosens. Bioelectron., 23 721 (2007).

[7] Z. Du, H. Li, T. Gu, Biotechnology Advances, 25, 464 (2007).

[8] A.L. Vázquez-Larios, E. Ríos-Leal, O. Solorza-Feria, H.M. Poggi-Varaldo, "X Congreso Internacional de la Sociedad Mexicana del Hidrógeno- Energías Renovables" y "IV Congreso Internacional de Uso Racional y Eficiente de la energía-CIUREE 2010", 2010.

[9] A.L. Vazquez-Larios, O. Solorza-Feria, G. Vazquez-Huerta, F. Esparza-Garcia, E. Rios-Leal, N. Rinderknecht-Seijas, H.M. Poggi-Varaldo, J. New Mat. Electrochem. Systems, 13, 219 (2010).

[10] D.Q. Jiang, B.K. Li, Water Sci. Technol., 59, 557 (2009).

[11] E.J. Rodríguez-Varela, O. Solorza-Feria, E. Hernández-Pacheco, "Celdas de combustible". Capítulo 7 1st edn., Canada, 2010.

[12] G.W. Castellan, "Physical Chemistry", 1st edn., 3rd printing, Addison-Wesley Publ. Co. Reading, MA, USA, 1969, p 594.

[13] Y. Guerasimov, V. Dreving, E. Eriomin, A. Kiseliov, V. Lebedev, G. Panchenkov, A. Shliguin, "Curso de Quimica-Física", Ed. MIR, Moscow, Volume 2, 1971, p 446.

[14] R.B. Bird, W.E. Stewart, E.N. Lightfoot, "Transport Phenomena". John Wiley & Sons, Inc., New York. Wiley International Edition, 1960, p 515.

[15] J.E. Bayley, D.F. Ollis, "Biochemical Engineering Fundamentals". 2nd edn., McGraw-Hill Publ. Co., New York, USA. 1986.

[16] B. Min, O.B. Román, I. Angelidaki, Biotechnol. Letters, 30, 1213 (2008).

[17] X. Wang, Y.J. Feng, H. Lee, Water Sci. Technol., 57, 1117 (2008).

[18] D. Halliday, R. Resnick, J. Walker, "Fundamentals of Physics", 7th ed. John Wiley & Sons Co., New York, 2004.

[19] I. Valdez-Vazquez, E. Ríos-Leal, F. Esparza-García, F. Cecchi, H.M. Poggi-Varaldo, Int. J. Hydrogen Energy, 30, 1383 (2005).

[20] H.M. Poggi-Varaldo, L. Valdés, G. Fernández-Villagómez, F. Esparza-García, Water Sci. Technol., 35, 197 (1997).

[21] R. Sparling, D. Risbey, H.M. Poggi-Varaldo, Int. J. Hydrogen Energy, 22, 563 (1997).

[22] APHA, "Standard Methods for the Examination of Water and Wastewater", American Public Health Association, Washington DC, USA, 1989.

[23] S.-J. You, N.-Q. Ren, Q.-L. Zhao, J.-Y.Wang, F.-L. Yang, Fuel Cells, 9, 588 (2009).

[24] H. Liu, S. Cheng, B.E. Logan, Environ. Sci. Technol., 39, 5488 (2005).

[25] T. Song, Y. Xu, Y. Ye, Y. Chen, S. Shen, J. Chem. Technol. Biotechnol., 84, 356 (2008).

[26] H. Liu, B.E. Logan, Environ. Sci. Technol., 38, 4040 (2004).

[27] S. Cheng, B.E. Logan. Electrochem. Commun., 9, 492 (2007).

[28] S.-E. Oh, B.E. Logan. Appl. Microbiol. Biotechnol., 70, 162 (2006).

[29] S. Cheng, H. Liu, B.E. Logan. Electrochem. Commun., 8, 489 (2006).

[30] H.J. Kim, H.S. Park, M.S. Huyun, I.S. Chang, M. Kim, B.H. Kim, Enzyme Microb., Technol., 30, 145 (2002).

[31] D.R. Bond, D.R. Lovley, Appl. Environ. Microbiol., 69, 1548 (2003).

[32] G. Reguer, K.D. McCarth, T. Meht, J.S. Nicol, M.T. Tuomine, D.R. Lovle, Nature, 435, 1098 (2005).

[33] A.C. Ortega Martínez, A.L. Vázquez Larios, K. Juárez-López, O. Solorza-Feria, H.M. Poggi-Varaldo, 14th Int. Biotechnol. Symp., Rimini, Italy (2010).